



# Utilization of Synchrotron Analysis in the Development of Compound Semiconductor Devices

Yoshihiro SAITO\*, Shigeaki UEMURA, Takumi YONEMURA,  
and Junji IIHARA

Compound semiconductors have beneficial features that enable high performance devices. In this study, we utilized synchrotron radiation x-ray photoelectron spectroscopy (XPS) techniques to precisely analyze semiconductor surface and interface states, which significantly affect device performance. Regarding gallium nitride high electron mobility transistor (GaN-HEMT) devices for wireless communication, x-ray energy was lowered to 600 eV to study the effect of the O<sub>2</sub> ashing process, achieving a probing depth of approximately 2 nm. Combined with photoluminescence analysis, it was confirmed that inappropriate process conditions increased the escape of nitrogen atoms, surface oxidation, and defects in GaN crystals. For the InP-based photodiodes used as detectors in optical communication, the surface potential of InP covered with dielectric films was evaluated, using hard x-ray photoemission spectroscopy with an excitation energy of 7940 eV. Based on our analysis, the film deposition condition was optimized and the leakage current at the interface was successfully reduced to obtain sufficiently high optical sensitivity. This study has demonstrated that timely utilization of synchrotron radiation analysis is extremely effective in shortening the product development of Sumitomo Electric Industries, Ltd.

Keywords: compound semiconductor device, GaN, InP, XPS, synchrotron analysis

## 1. Introduction

Compound semiconductors such as gallium nitride (GaN) and indium phosphate (InP) have been widely used in wireless and optical communication systems due to their beneficial features for high performance devices that cannot be realized by silicon (Si). In the manufacturing processes of these devices, however, there are some difficulties that also derive from their material properties. For instance, atomic composition at the semiconductor surface can easily change depending on process conditions. To achieve a high yield in manufacturing, it is important to precisely analyze the states of the semiconductor surface and interface covered with passivation films.

Among the various kinds of surface analysis techniques, one of the most popular is x-ray photoelectron spectroscopy (XPS), which enables us to quantitatively probe surface composition and chemical bonding. As for x-ray sources, in addition to conventional x-ray tubes, synchrotron radiation\*<sup>1</sup> is also useful, since it can tune the x-ray energy corresponding to the desired probing depth. In this study, we used synchrotron radiation XPS analysis in the development of our compound semiconductor devices.

## 2. Features and Problems of Compound Semiconductor Devices

Figure 1 shows some examples of the compound semiconductor devices released by Sumitomo Electric Industries, Ltd. As for GaN high electron mobility transistors (GaN-HEMTs), which can realize 100 W class output power at frequencies higher than 3 GHz, demand is expanding in 5G base stations in wireless communication

systems.<sup>(1),(2)</sup> The wide bandgap of GaN-based semiconductors compared to that of Si is very suitable for high output power. High electron mobility, which is achieved by employing an AlGaIn/GaN hetero epitaxial structure channel, is indispensable in realizing high frequency operation.

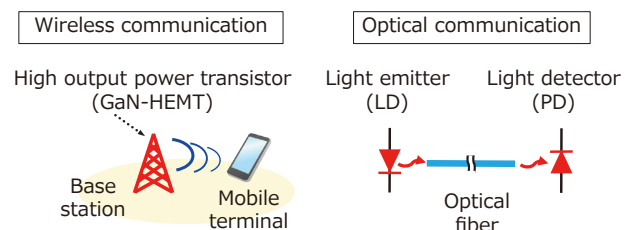


Fig. 1. Sumitomo Electric's compound semiconductor device products

In optical communication, InP-based laser diodes (LDs) and photodiodes (PDs) are used as light emitting and detecting devices, respectively.<sup>(3)-(5)</sup> It is well-known that the transmitting length in an optical fiber reaches its maximum at a wavelength of 1.55  $\mu\text{m}$ . To realize high emission or detection efficiencies around that wavelength, mixed crystals composed of indium, gallium, arsenic, and/or phosphine, which can be epitaxially grown on InP substrates, are necessary.

As described above, the features of compound semiconductor materials offer great advantages in the realization of high-performance devices. However, there are some difficulties that also come from their properties. For

instance, the surface state of GaN and InP can be easily changed by oxidation and atomic composition deviation, as shown in Fig. 2.<sup>(6)</sup>

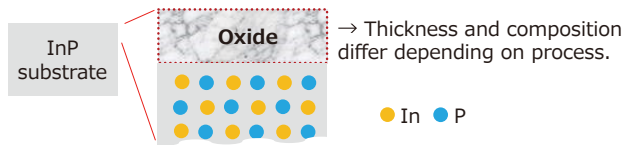


Fig. 2. Schematic cross section of InP surface

Another problem is the passivation film for the semiconductor surface. For Si, very high quality SiO<sub>2</sub> passivation films with low defect density can be formed by the thermal oxidation process. On the other hand, it is necessary to employ a deposition process such as plasma-enhanced chemical vapor deposition (PECVD) to passivate compound semiconductor surfaces. Inappropriate deposition conditions may degrade the quality of the interface, which significantly affects both device performance and reliability. Therefore, it is of importance to develop technologies to analyze them precisely.

### 3. Synchrotron Radiation XPS

In XPS analysis, irradiation of x-ray onto a material generates photoelectrons, the kinetic energy ( $E_k$ ) of which is measured. The difference between the x-ray energy ( $h\nu$ ) and  $E_k$  is called binding energy ( $E_b$ ), which shifts depending on the chemical state of atoms in the material. Figure 3 shows an example of the P2p XPS spectrum, obtained from an InGaAsP mixed crystal with an approximately 1 nm thick oxide on its surface. It is recognized that the  $E_b$  of P-O in the oxide is higher than that of P-In and P-Ga in an InGaAsP by 4 eV. This is caused by the high electronegativity of the O atoms, which makes it difficult for electrons to escape from the P atoms. The change of  $E_b$  is called chemical shift.

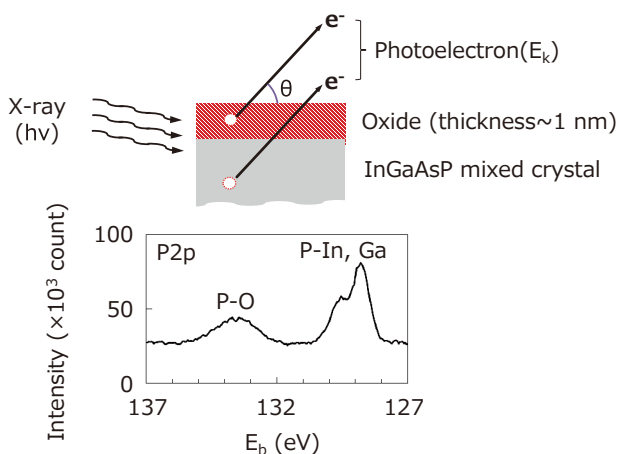


Fig. 3. P2p XPS obtained from InGaAsP

The probing depth ( $d$ ) in XPS analysis is expressed by the following equation:  $d = 3\lambda \cdot \sin\theta$ , where  $\lambda$  and  $\theta$  are inelastic mean free path and take-off angle, respectively.<sup>(7)</sup>  $\theta$  is the angle formed by the sample surface and photoelectron trajectory, as indicated in Fig. 3. Basically, the higher the  $h\nu$ , the larger the  $\lambda$  and the  $d$ . Regarding the contribution of  $\theta$ ,  $d$  increase as  $\theta$  gets close to 90 degrees, since the path length for photoelectrons within the sample becomes shorter. The  $h\nu$  and  $\theta$  should be selected corresponding to the desired  $d$ .

Figure 4 shows the  $d$  of N1s in GaN, which was calculated based on the TPP-2M theory.<sup>(8)</sup> To precisely analyze the very surface region where oxidation and/or N atom escape occurs, the suitable  $h\nu$  and  $\theta$  are found to be 600 eV and 30 to 85 degrees, respectively. In the case of Al-K $\alpha$  line (1487 eV), which is often used in commercially available x-ray tubes, it is very difficult to make  $d$  smaller than 2 nm, due to the relatively large number of photoelectrons from the deeper region. Note that employing a small  $\theta$  such as 10 degrees is not very useful to lower  $d$ , since the photoelectrons from the deeper region can mix by elastic scattering.<sup>(9)</sup>

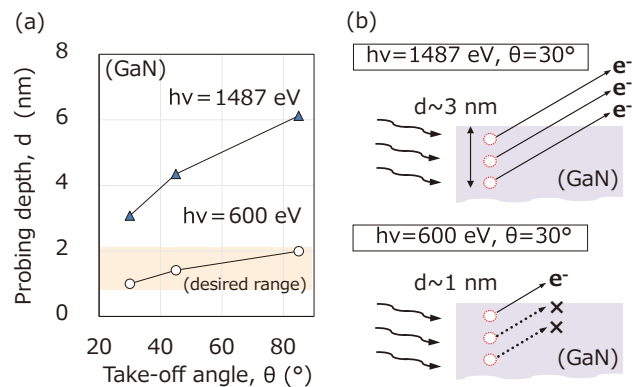


Fig. 4. Probing depth of N1s in GaN

On the contrary, to analyze the interface between a semiconductor substrate and passivation film, relatively high  $h\nu$  is preferable. Figure 5 shows the calculated  $d$  for In<sub>3d<sub>3/2</sub></sub> in InP covered with a 10 nm thick silicon nitride (SiN<sub>x</sub>) film. It was demonstrated that  $h\nu$  of 1487 eV is not sufficiently high for the photoelectrons from the In atoms

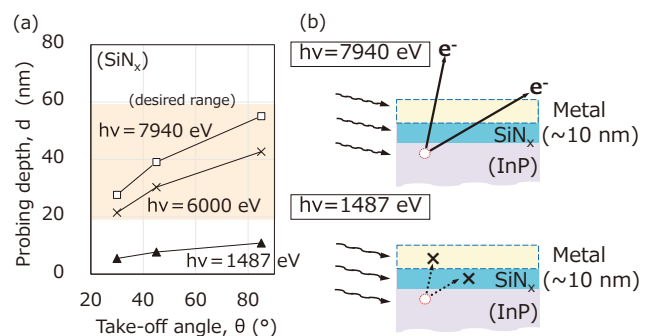


Fig. 5. Probing depth of In<sub>3d<sub>3/2</sub></sub> in SiN<sub>x</sub>

to pass through the SiN<sub>x</sub> film, even at θ of 85 degrees. Besides, it is usually necessary to deposit a several nm thick metal layer to reduce the charge up during measurement. In this case, the so-called hard x-ray photoemission spectroscopy (HAXPES) technique with excitation energy higher than 6000 eV is useful.<sup>(10)</sup>

### 4. Experiments and Results

#### 4-1 GaN surface

Figure 6 shows an example of the fabrication process to form the gate electrode in a GaN-HEMT, which starts with SiN<sub>x</sub> film deposition and photoresist mask patterning. Then, the SiN<sub>x</sub> film is etched by reactive ion etching (RIE) and organic contaminations are removed by O<sub>2</sub> ashing\*<sup>2</sup>. To solve the oxides on the GaN surface generated in the ashing process, cleaning in hydrochloric acid (HCl) solution is carried out. Finally, the electrode metal is evaporated.

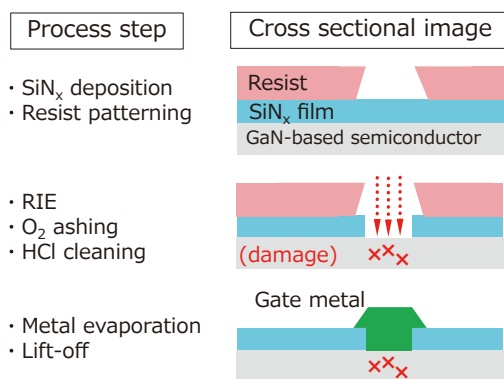


Fig. 6. Fabrication of gate electrode in GaN-HEMT

Generally, in plasma processes such as RIE and O<sub>2</sub> ashing, inappropriate process conditions may cause some damage to the semiconductor surface and degrade device performance. In this study, focusing on the effect of O<sub>2</sub> ashing on the GaN surface, samples for XPS analysis were prepared, as illustrated in Fig. 7. Epitaxially grown GaN

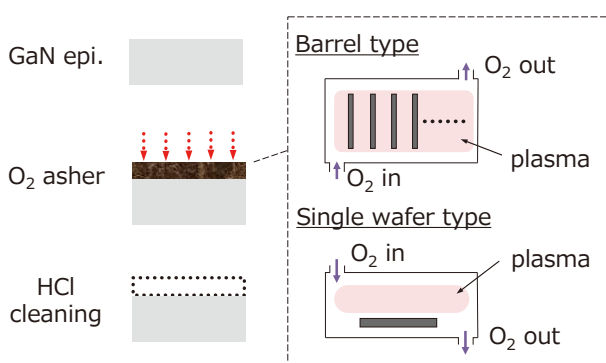


Fig. 7. Analysis samples of GaN surface

substrates went through O<sub>2</sub> ashing and HCl cleaning. For the ashing step, two types of equipment were employed: one was a conventional barrel type asher and the other was a single wafer process type asher with a higher ashing rate.

The XPS measurements were done in SAGA-LS\*<sup>3</sup>, Japan, at BL17 that was installed by Sumitomo Electric. The incident x-ray energy was tuned to 600 eV. Figure 8 (a) shows examples of Ga3d and N1s spectra, obtained at θ of 45 degrees. The ascending order of the peak intensity ratio of N1s to Ga3d, which gets smaller as more N atoms escape from the GaN surface, was found to be single wafer type asher, barrel type asher, and reference sample. In particular, ashing in the single wafer equipment resulted in an extremely low N1s intensity, indicating that almost all the N atoms escaped from the GaN surface region.

As for the quantity of oxide on the GaN surface, it was very difficult to separate the peak of Ga-O from that of Ga-N by fitting, since their peak positions were very close to each other. It was considered that the oxide on the GaN surface was not Ga<sub>2</sub>O<sub>3</sub> but Ga<sub>2</sub>O. However, it was recognized that the full width at half maximum (FWHM) of the whole Ga3d peak became larger as the surface oxide increased. The obtained descending order of the FWHM was single wafer type asher, barrel type asher, and reference sample. In Fig. 8 (b), the FWHMs are plotted versus the N/Ga peak intensity ratios, demonstrating that surface oxide generated by the ashing processes was not removed completely by HCl cleaning.

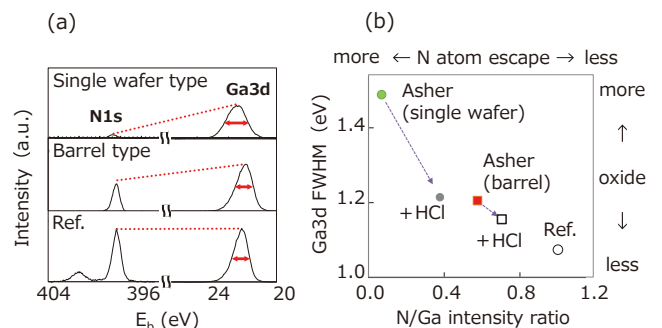


Fig. 8. (a) XPS measurement examples for GaN (b) Ga3d FWHM vs N1s/Ga3d intensity ratio

To investigate the relationship between process conditions and defect generation in GaN crystals, photoluminescence (PL) analysis was also carried out. As shown in Fig. 9 (a), there are two peaks in a PL spectrum from GaN, with an excitation light wavelength of 325 nm. One is the sharp peak at 360 nm that corresponds to the band edge emission (I<sub>band</sub>). The other is the broad peak around 600 nm, which is derived from the defects in GaN crystals and called “Yellow Luminescence (YL)”<sup>(11)</sup>. The peak intensity ratio, I<sub>YL</sub>/I<sub>band</sub>, stands for the normalized quantity of defects. The descending order of the quantity of defects was confirmed to be single wafer type asher, barrel type asher, and reference sample, as shown in Fig. 9 (b).

Figure 10 shows the relationship between the I<sub>YL</sub>/I<sub>band</sub> intensity ratios and N/Ga intensity ratios. The square of

correlation coefficient between them was as high as 0.94. From these results, it was demonstrated that neither the surface state of GaN nor defects in the GaN crystal recovered to the same level as the reference sample even after HCl cleaning.

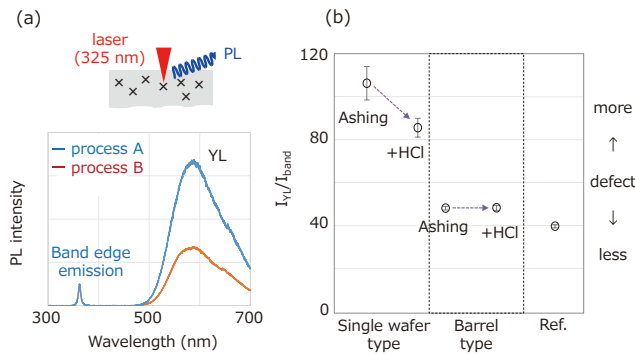


Fig. 9. (a) PL measurement examples of GaN (b)  $I_{YL}/I_{band}$  of GaN samples

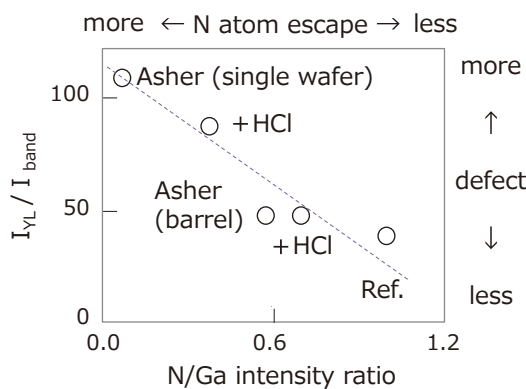


Fig. 10.  $I_{YL}/I_{band}$  (PL) vs N1s/Ga3d ratio (XPS)

One of the possible mechanisms suggested from the results described so far is shown in Fig. 11. In the reference sample, very slight native oxide exists on the GaN surface.

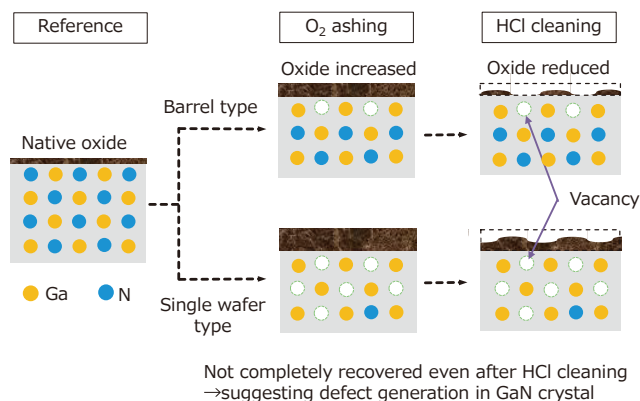


Fig. 11. Effect of O<sub>2</sub> ashing on GaN surface: possible mechanism

The O<sub>2</sub> ashing process grows the oxide that cannot be removed completely by HCl cleaning. The ashing process also increases the defects in the GaN crystal. Though a possible candidate for the defects is thought to be an N vacancy, additional analysis is necessary to identify that. Regarding the ashing equipment, the single wafer type asher grows more oxide and defects than the barrel type asher. Though the whole mechanism has not been clarified yet, synchrotron radiation XPS analysis combined with PL has been found to be very useful to quantitatively analyze process performance.

#### 4-2 SiN<sub>x</sub>/InP interface

As for the InP-based PD device for optical communication, we investigated the state of the interface between the SiN<sub>x</sub> film and InP substrate, which significantly affects the sensitivity as a light detector. Figure 12 illustrates the relationship between the leakage current at the interface and the sensitivity of PD. Absorption of an optical signal by the PD generates electron-hole pairs that lowers electrical resistance. The increase of current in the PD converts the optical signal to an electrical one. Assuming an ideal interface state between the SiN<sub>x</sub> film and InP substrate, the current in the PD becomes almost zero when no signal arrives. However, if process conditions are not sufficiently sophisticated, non-negligible leakage current flows at the interface even when no optical signal arrives, which results in degradation of the sensitivity.

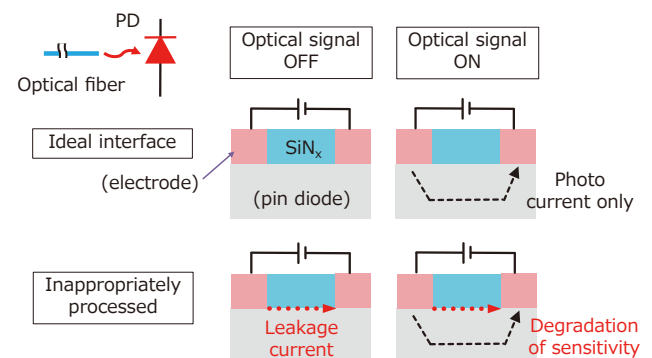


Fig. 12. Effect of leakage current at SiN<sub>x</sub>/InP interface on light sensitivity of InP-based PD

Though the leakage current is affected by both wet cleaning of the InP surface and deposition of SiN<sub>x</sub> film, we focused on the latter in this study. As for the analysis samples, SiN<sub>x</sub> films were deposited on InP substrates, using conventional parallel plate type PECVD. Among the employed conditions, the deposition rate of #1 was one order of magnitude larger than those of #2 and #3. Then, aurum (Au) was evaporated on the SiN<sub>x</sub> films, to reduce charge-up during the HAXPES measurements. The thickness of each layer was 10 nm.

The HAXPES measurements were carried out at BL16XU in SPring-8<sup>4</sup>. The incident x-ray energy was 7940 eV. Since a slight shift of E<sub>b</sub> was observed due to charge up in each sample, all the measured data were calibrated so that the peak position of Au4f<sub>7/2</sub> would be the



original point or 84 eV. The results are shown in Fig. 13. It was confirmed that the  $E_{bs}$  of  $In3d_{3/2}$  and  $P1s$  of sample #1 were higher than those of #2 and #3 by approximately 0.2 eV. This was caused by the lowering of the InP surface potential at the interface, which should increase the leakage current.

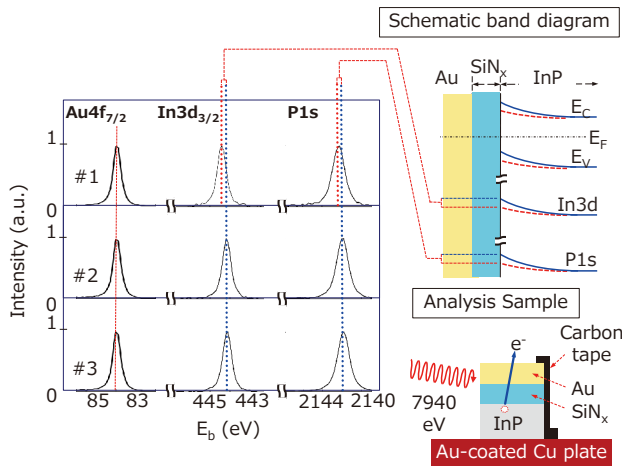


Fig. 13. Results of HAXPES analysis for  $SiN_x/InP$  interfaces

Besides the HAXPES analysis, PD devices were also fabricated employing PECVD  $SiN_x$  films. The results are summarized in Table 1. The measured leakage current of the PDs fabricated using conditions #2 and #3 were two orders of magnitude lower than that of PDs using condition #1, demonstrating that the prediction from the HXAPES analysis was correct.

Table 1. InP peak shift and leakage current of PD

Sample	HAXPES: Peak shift* ( $In3d_{3/2}$ and $P1s$ )	Leakage current of PD ** ( $\mu A$ )
#1	+0.2 eV	39.15 (15.00)
#2	0.0 eV	0.69 (0.24)
#3	0.0 eV	0.75 (0.34)

\*) Difference from measured data for #3

\*\*) Average of 140 points in wafer (Standard deviations in blanket)

### 5. Shortening Product Development by Utilization of Analysis

Generally, the manufacturing of semiconductor devices involves many processes, which often makes the lead time longer than one month. Therefore, if we attempt to optimize each process condition by repeating the cycle of device fabrication and characterization, development time becomes extremely long. However, the utilization of analysis techniques to associate the process parameters with device characteristics can shorten development time, as shown in Fig. 14.

Synchrotron radiation, which was utilized to analyze the GaN surface and  $InP/SiN_x$  interface in this study, enables us to obtain precious knowledge that cannot be

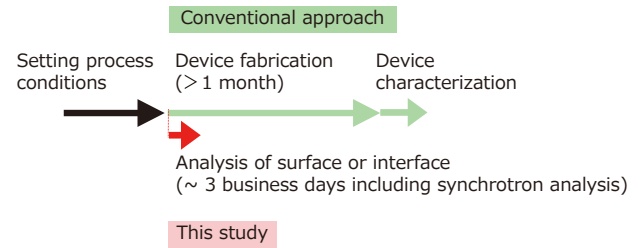


Fig. 14. Shortening product development by utilization of analysis techniques

obtained without difficulty as long as commercially available analysis equipment alone is used. Usually, to perform synchrotron analysis, it is necessary to submit a proposal to beamlines for common use installed in accelerator facilities. Sometimes it takes several months to gain acceptance for the proposal and to carry out the synchrotron analysis.

As described previously, Sumitomo Electric installed two beamlines\*<sup>5</sup> in SAGA-LS and started operation in November 2016, in order to secure machine time for various kinds of x-ray analysis including XPS. Sumitomo Electric has also been a member of Sunbeam or the Industrial Consortium in SPring-8, utilizing hard x-ray analysis. Due to the beamlines in SAGA-LS and SPring-8, we can use the synchrotron radiation analysis in a timely manner, which has proven to be extremely effective in shortening the product development.

### 6. Conclusion

The states of compound semiconductor surfaces and interfaces were analyzed, using synchrotron radiation XPS techniques. As for the GaN-HEMTs, the effect of the  $O_2$  ashing process on the GaN surface was investigated, by lowering the x-ray energy to 600 eV to achieve a probing depth of approximately 2 nm. Combined with PL analysis, it was confirmed that inappropriate process conditions increased the escape of N atoms, surface oxidation, and defects in GaN crystals. Regarding InP-based photodiodes, the surface potential of InP covered with  $SiN_x$  passivation films was evaluated, using the HAXPES technique with an excitation energy of 7940 eV, to search appropriate  $SiN_x$  deposition conditions. The results of the PD fabrication were found to be consistent with those of the analysis and the leakage current at the  $InP/SiN_x$  interface was successfully reduced. The timely utilization of synchrotron radiation analysis proved to be very effective in shortening product development of Sumitomo Electric.

### 7. Acknowledgements

The XPS measurements were performed at BL17 of SAGA-LS (Proposal No. SEI2020B-006, SEI2021B-006). The HAXPES experiments were conducted at BL16XU of SPring-8 with the approval of the Japan Synchrotron Radiation Research Institute (JASRI, Proposal No.: 2019B5030). The authors wish to thank everyone involved for their assistance.

### Technical Terms

- \*1 Synchrotron radiation: Extremely high intense white electromagnetic waves, generated in the tangential direction by bending the orbits of electrons that are in motion at velocities close to that of light.
- \*2 O<sub>2</sub> ashing: Process to oxidize and remove organic materials such as photoresists, by exposure to O<sub>2</sub> plasma.
- \*3 SAGA-LS: The synchrotron radiation facility in Tosu City, established by the Saga Prefectural Government and operated by Saga Product Promotion Public Corporation. It came into service in 2006. SAGA-LS is the abbreviation for SAGA Light Source and the official name is the Kyushu Synchrotron Light Research Center. The stored electron energy in the ring is 1.4 GeV.
- \*4 SPring-8: One of the world's largest synchrotron radiation facilities, located in Harima Science Garden City in Hyogo Prefecture, Japan. The name is derived from "Super Photon ring-8 GeV" and the stored electron energy in the ring is 8 GeV. It came into service in 1997.
- \*5 Sumitomo Electric Beamline: Beamlines for soft and hard x-rays installed in SAGA-LS by Sumitomo Electric. They started operation in November 2016. Synchrotron analysis is conducted for about 3000 hours a year in total, using the two beamlines.

### References

- (1) K. Inoue\*, S. Sano, Y. Tateno, F. Yamaki, K. Ebihara, N. Ui, A. Kawano, and H. Deguchi, "Development of Gallium Nitride High Electron Mobility Transistors for Cellular Base Stations," SEI TECHNICAL REVIEW No. 71, pp. 88-93 (2010)
- (2) S. Sano\*, K. Ebihara, T. Yamamoto, T. Sato, and N. Miyazawa, "GaN HEMTs for Wireless Communication," SEI TECHNICAL REVIEW No. 86, pp. 65-70 (2018)
- (3) T. Katsuyama, "Development of Semiconductor Laser for Optical Communication," SEI TECHNICAL REVIEW No. 69, pp. 13-20 (2009)
- (4) M. Honda, A. Tamura, K. Takada, K. Sakurai, H. Kanamori, and K. Yamaji, "53 GBaud Electro-Absorption Modulator Integrated Lasers for Intra-Data Center Networks," SUMITOMO ELECTRIC TECHNICAL REVIEW No. 96, pp. 20-24 (2023)
- (5) T. Okimoto, K. Ebihara, K. Yamazaki, S. Okamoto, H. Yagi, and Y. Yoneda, "InP-based Photodiodes Integrated with Optical Mixer for 800 Gbit/s Coherent Transmission," SUMITOMO ELECTRIC TECHNICAL REVIEW No. 93, pp. 7-12 (2021)
- (6) Y. Saito, S. Uemura, T. Kagiya, R. Toyoshima, "XPS and HAXPES analyses for pre-sputtered InP surface and InP/Pt interface," Jpn. J. Appl. Phys., vol35, pp31005(1)-(5) (2022)
- (7) K. Tanak, "X-Ray Photoelectron Spectroscopy: XPS", [https://www.spsj.or.jp/equipment/news/news\\_detail\\_73.html](https://www.spsj.or.jp/equipment/news/news_detail_73.html)
- (8) H. Shinotsuka, S. Tanuma, C. J. Powell, and D. R. Penn, "Calculations of electron inelastic mean free paths. X. Data for 41 elemental solids over the 50 eV to 200 keV range with the relativistic full Penn algorithm," Surf. Interface Anal., vol 47, pp871-888 (2015)
- (9) Thermo Fisher Scientific, "Angle Resolved XPS," Application Note: 31014, p7 (2008)  
<https://assets.thermofisher.com/TFS-Assets/CAD/Application-Notes/D16069-.pdf>
- (10) M. Kobata and K. Kobayashi, "Study of Oxide Film with the Hard X-ray Photoelectron Spectroscopy," J. Vac. Soc. Jpn., Vol. 58, No. 2, pp43-49, (2015)
- (11) M. Reshchikova and Hadis Morkoç, J. Appl. Phys., vol97, 061301 (2005)

### Contributors

The lead author is indicated by an asterisk (\*).

#### Y. SAITO\*

- Doctor of Engineering
- Senior Specialist
- Analysis Technology Research Center



#### S. UEMURA

- Doctor of Science
- Assistant General Manager, Analysis Technology Research Center



#### T. YONEMURA

- Assistant Manager, Analysis Technology Research Center



#### J. IIHARA

- Doctor of Science
- Group Manager, Analysis Technology Research Center

